JACS
JOURNAL OF THE AMERICAN CHEMICAL SOCIETY

Communication

pubs.acs.org/JACS

Efficient Tandem and Triple-Junction Polymer Solar Cells

Weiwei Li, Alice Furlan, Koen H. Hendriks, Martijn M. Wienk, and René A. J. Janssen*

Molecular Materials and Nanosystems, Eindhoven University of Technology, P.O. Box 513, 5600 MB Eindhoven, The Netherlands

Supporting Information

ABSTRACT: We demonstrate tandem and triple-junction polymer solar cells with power conversion efficiencies of 8.9% and 9.6% that use a newly designed, high molecular weight, small band gap semiconducting polymer and a matching wide band gap polymer.

Solution-processed organic and polymer solar cells attract considerable interest because they offer the prospect of high-efficiency, flexible devices combined with cheap roll-to-roll processing. A widespread material combination is a mixture of a conjugated polymer as electron donor and a fullerene acting as electron acceptor. Power conversion efficiencies (PCEs) have increased significantly over the past years, now reaching over 9%.[1] Further improvements are required, and these can be found in extending the spectral coverage of the solar cells to the near-infrared (NIR). As an example, the highest efficiency organic solar cell published to date converts light up to wavelengths of ∼780 nm but is not yet able to exploit the NIR light of the sun.[1] Although several small band gap semiconducting polymers have been developed that absorb NIR light,[2−6] their performance in photovoltaic devices has been unsatisfactory in terms of reaching high PCEs, because either their external quantum efficiency (EQE) for photon-to-electron conversion is modest or the open-circuit voltage (V_{oc}) of the cells is reduced in consequence of the small band gap.

A successful and universal strategy to increase the performance of solar cells and extend their spectral coverage is to use tandem configurations. In these double-junction cells, photons with high and low energy are spatially separated and absorbed in the photoactive layers that have complementary band gaps to reduce thermalization and transmission losses that are inevitable in a single-junction device. Recently several polymer−fullerene tandem solar cells have been developed that outperform the single-junction cells made with the same absorber materials.[7−11] The best polymer−fullerene tandem solar cells have an efficiency of 10.6%[11] and feature a response up to ∼900 nm. While the response is shifted significantly compared to those of the best single junctions, further progress hinges on new materials with extended spectral coverage that are optimized for application in tandem solar cells.

Here we report the design and synthesis of a new small band gap semiconducting polymer, poly[[2,5-bis(2-hexyldecyl-2,3,5,6-tetrahydro-3,6-dioxopyrrolo[3,4-*c*]pyrrole-1,4-diyl]-*alt*-[3′,3″-dimethyl-2,2′:5′,2″-terthiophene]-5,5″-diyl] (PMDPP3T, Figure 1) that absorbs well into the NIR region. We demonstrate that photovoltaic cells comprising active layers of PMDPP3T blended with [6,6]-phenyl-C_{71}-butyric acid methyl ester ([70]PCBM) reach a maximum PCE of 7.0% in single-junction cells, with a high photoresponse up to 960 nm. Moreover, sub-cells of PMDPP3T with [6,6]-phenyl-C_{61}-butyric acid methyl ester ([60]PCBM) provide very efficient tandem and triple-junction cells with broad spectral response and PCEs of 8.9% and 9.6% when combined with a wide band gap sub-cell consisting of poly[[9-(1-octylnonyl)-9*H*-carbazole-2,7-diyl]-2,5-thiophenediyl-2,1,3-benzothiadiazole-4,7-diyl-2,5-thiophenediyl] (PCDTBT, Figure 1)[12,13] and [70]PCBM. The high complementarity of the absorption spectra of the active layers (see Supporting Information (SI) Figure S2) makes it possible to achieve high photocurrents in tandem and triple configurations.

Figure 1. Molecular structures of the new near-infrared-absorbing copolymer PMDPP3T and of PCDTBT.

The new copolymer was designed to comprise diketopyrrolopyrrole (DPP) as an electron-poor conjugated unit alternating with a terthiophene unit as electron-rich fragment. DPP has emerged as a versatile building block in combination with electron-rich fragments such as oligothiophenes to yield efficient small band gap donor polymers for polymer solar cells.[14−16] The band gap of DPP polymers can be effectively tuned by the length of the electron-rich fragments connecting the DPP units.[17] Reducing the number of thiophene rings from six to three reduces the gap by 0.18 eV.[17] To date PDPP3T, which incorporates unsubstituted terthiophene units alternating with DPP, is one of the most efficient polymers with a sufficiently small band gap (1.30 eV).[18,19] The new polymer, PMDPP3T, bears two additional methyl substituents on the 3-position of the thiophene rings connected to the DPP fragment to bring about an inductive electron-donating effect that raises the energy levels of frontier orbitals of PMDPP3T compared to PDPP3T, without introducing any additional steric effects that could affect the solid-state properties of the material.[20,21] The rise of the energy levels enhances the driving force for photoinduced electron transfer to [60]PCBM and [70]PCBM, which contributes to an increased photocurrent. PMDPP3T was synthesized by a Stille-type cross-coupling polymerization reaction from the corresponding monomers, yielding a material with a high molecular weight of M_n = 110 kg mol^{-1} and M_w =

Received: February 7, 2013
Published: April 2, 2013

   dx.doi.org/10.1021/ja401434x | *J. Am. Chem. Soc.* 2013, 135, 5529−5532

282 kg mol^{-1} (see SI and Figure S3). The effect of the methyl substituents on the optical absorption properties is minimal: the optical band gap of a solid film, determined from the absorption onset of PMDPP3T (E_g = 1.30 eV), is identical to that of PDPP3T. Charge carrier mobilities were determined using a field-effect transistor (FET) with a bottom gate–bottom contact configuration. PMDPP3T displays ambipolar behavior with balanced hole and electron mobilities in the range of 10^{-2}–10^{-3} cm^2 V^{-1} s^{-1}, very similar to PDPP3T.[18] The onset of the electrochemical reduction, which is related to the energy level of the lowest unoccupied molecular orbital (LUMO), is shifted to more negative values by ∼70 mV for PMDPP3T compared to PDDP3T, as determined by cyclic voltammetry (Figure S4), as a consequence of the electron-donating effect of the methyl substituents.

Single-junction solar cells were made with PMDPP3T:[70]PCBM blends on patterned indium tin oxide (ITO) glass substrates covered with a thin poly(3,4-ethylenedioxythiophene):poly(styrenesulfonate) (PEDOT:PSS) layer and using a LiF/Al back contact. Cells were optimized in terms of polymer:fullerene ratio, type and amount of processing cosolvent, and layer thickness (see SI). The current density–voltage (J–V) characteristics and spectrally resolved EQE are displayed in Figure 2, and the results are summarized in Table

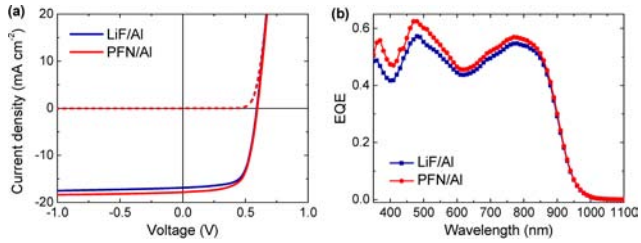

Figure 2. (a) J–V and (b) EQE of single-junction PMDPP3T:[70]PCBM cells with LiF/Al and PFN/Al back contacts under simulated AM1.5G illumination.

Table 1. Characteristics of Optimized Single-Junction Solar Cells

acceptor	contact	J_{sc}[a] (mA cm^{-2})	V_{oc} (V)	FF	PCE[a] (%)
[70]PCBM	LiF/Al	16.9	0.59	0.68	6.8
[70]PCBM	PFN/Al	17.8	0.60	0.66	7.0
[60]PCBM	LiF/Al	14.8	0.61	0.65	5.8
[60]PCBM	PFN/Al	16.1	0.61	0.64	6.2

[a] J_{sc} was calculated by integrating the EQE spectrum with the AM1.5G spectrum.

1. The highest PCE of 6.8% was achieved using PMDPP3T and [70]PCBM in a 1:3 weight ratio, deposited from a mixture of chloroform and *o*-dichlorobenzene (*o*-DCB). The devices provide a high short-circuit current density (J_{sc}) of 16.9 mA cm^{-2} and a concomitantly high EQE. The EQE reaches unprecedentedly high levels for a polymer solar cell absorbing in the NIR region: at 800 nm, EQE = 0.55, and even at 900 nm an EQE > 0.20 is obtained. In addition, the fill factor (FF = 0.68) is also very high, indicating efficient charge carrier collection, even at low electric fields over the absorber layer. The V_{oc} of 0.59 V for PMDPP3T devices is lower than the value obtained for PDPP3T (V_{oc} = 0.66 V).[18,19] The magnitude of this V_{oc} reduction is in line with the eletrochemically determined increase of the frontier orbital levels. Still, for PMDPP3T:[70]PCBM the increased J_{sc} and FF greatly outweigh this voltage loss, and the overall PCE is very high for such small band gap organic absorber. Further improvements of the device performance were achieved by replacing LiF at the electron-collecting aluminum contact by a thin poly[(9,9-bis(3′-(*N*,*N*-dimethylamino)propyl)-2,7-fluorene)-*alt*-2,7-(9,9-dioctylfluorene)] (PFN) polyelectrolyte layer.[1,22–24] This improved the J_{sc} to 17.8 mA cm^{-2}, mainly owing to an increased quantum efficiency in the [70]PCBM absorption range, and the V_{oc} to 0.60 V, yielding PCE = 7.0%. Compared to PDPP3T,[18,19] PMDPP3T provides a significant increase in EQE in the NIR (see SI for detailed comparison), which makes PMDPP3T a very attractive material for the back cell of a multi-junction solar cell in a two-terminal series connection. For the construction of tandem cells PMDPP3T was combined with PCDTBT,[12,13] which is one of the most efficient wide band gap conjugated polymers and has previously been used as a visible absorber in tandem cells.[25] PMDPP3T and PCDTBT have largely complementary absorption spectra, and to further minimize unfavorable absorption of high-energy photons by the small band gap back cell, it is advantageous to use [60]PCBM as electron acceptor molecule in combination with PMDPP3T. We found that optimized PMDPP3T:[60]PCBM devices display even higher EQEs than devices with [70]PCBM, reaching 61% in the polymer absorption maximum for devices with a LiF/Al back contact and 65% when PFN/Al is used. The overall PCE is 5.8% for cells with a LiF/Al contact and 6.2% for cells using PFN instead of LiF (Table 1 and Figure S5). This is lower than for the optimized [70]PCBM devices due to the reduced absorption in the visible range.

For constructing tandem cells (Figure 3a), the PMDPP3T:[60]PCBM sub-cell was combined with a front cell consisting of PCDTBT:[70]PCBM. The recombination layer between the two sub-cells consists of ZnO nanoparticles[26] as electron transport layer and pH-neutral PEDOT:PSS as hole transport layer.[8] No PFN layers were used. To determine the optimal thickness of the front and back sub-cells, optical and electrical modeling was used.[8] Based on the optical properties (i.e., the wavelength-dependent refractive index and extinction coefficient of all layers in the device) and the measured performance of a range of single-junction cells, and assuming no losses at the recombination contact, PCEs > 8.0% are expected for a broad range of tandem cells, with a front cell thickness between 140 and 180 nm and a back cell thickness between 130 and 170 nm (Figure S10). The highest efficiency of 8.5% is anticipated for a front cell of 155 nm and a back cell of 150 nm.

Tandem solar cells were made with these optimized sub-cell thicknesses and characterized under simulated solar illumination (Figure 3b). All efficiencies were above 8.4%, with a record cell of 8.9%. Compared to the corresponding wide band gap (PCDTBT:[70]PCBM 155 nm) and small band gap (PMDPP3T:[60]PCBM 150 nm) single-junction cells that provide PCE = 4.7% and 6.0%, respectively (Table 2 and Figure S11), the optimized tandem cell with the same layers and thickness has PCE = 8.9%, which represents an unparalleled increase of about 50%. Remarkably, the highest measured efficiency is higher than the predicted value, mainly resulting from a higher FF; the measured V_{oc} (1.49 V) and J_{sc} (9.6 mA cm^{-2}) correspond very well to the values predicted from optical

dx.doi.org/10.1021/ja401434x | J. Am. Chem. Soc. 2013, 135, 5529–5532

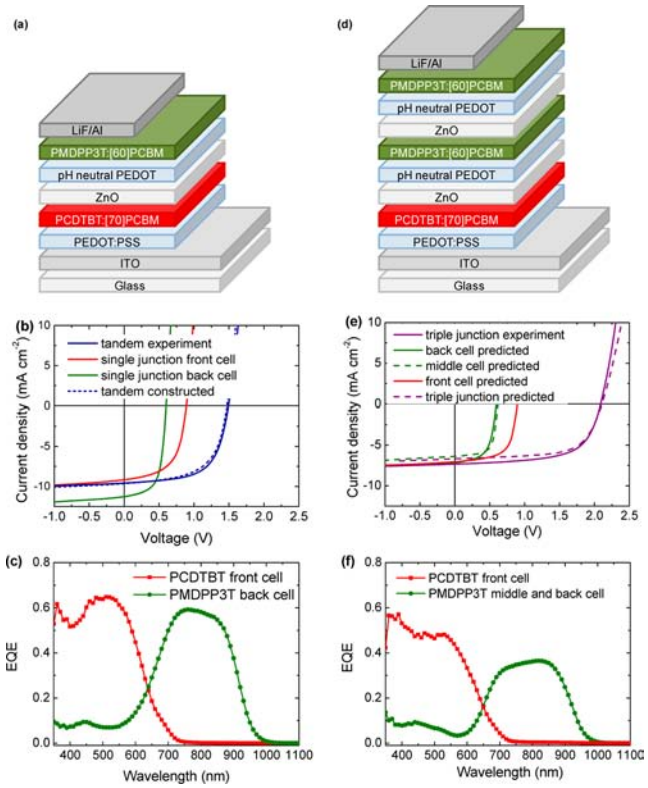

Figure 3. Tandem and triple-junction cells: (a,d) device layout, (b,e) $J-V$ characteristics, and (c,f) EQE measured under relevant bias illumination conditions and correct electrical bias. Panel b shows the $J-V$'s of the corresponding single-junction cells under reduced light intensity so that their J_{sc} corresponds to the value integrated from the EQEs shown in panel c.

Table 2. Characteristics of Tandem and Triple-Junction Solar Cells

device	J_{sc}[a] (mA cm^{-2})	V_{oc} (V)	FF	PCE[a] (%)
tandem predicted	9.53	1.50	0.59	8.46
tandem measured	9.58[a]	1.49	0.62	8.90
tandem constructed	9.64	1.48	0.59	8.44
PCDTBT:[70]PCBM[b]	9.76[a]	0.87	0.56	4.73
PMDPP3T:[60]PCBM[b]	15.30	0.61	0.65	6.00
triple predicted	6.68	2.10	0.65	9.20
triple measured	7.34[a]	2.09	0.63	9.64

[a] J_{sc} was measured under simulated solar light (100 mW cm^{-2}) tuned to the specific spectral sensitivities of the sub-cells (see SI for details). [b] Single-junction cells at layer thickness used in the tandem.

and electrical modeling (Table 2). For all measured devices the FF was higher than anticipated; the origin of this enhancement is currently still unclear.

EQE measurements of the individual sub-cells under relevant illumination conditions and correct electrical bias (see ref 27 and SI for details) reveal high quantum efficiencies with maxima of 64% for the front cell and 59% for the back cell (Figure 3c). We note that these EQEs are very similar to the EQE = 63% found for both single-junction cells at the same thickness. This demonstrates that the two absorber layers in the tandem cell are spectrally highly complementary. Integration of the EQE with the AM1.5G solar spectrum affords the current generation in each sub-cell, which is particularly high for the PMDPP3T:[60]PCBM back cell because it can deliver more than 11 mA cm^{-2}. The current generation in the PCDTBT:[70]PCBM front cell amounts to 9.2 mA cm^{-2}, which is higher than the value previously obtained for an optimized front cell of the same photoactive layer, but combined with a less red-shifted back cell,[25] as a consequence of the increased spectral complementarity.

The J_{sc} of the tandem cell measured under simulated solar light is 0.4 mA cm^{-2} higher than the current generation in the limiting front sub-cell. This is caused by the fact that the unbalanced current generation between the sub-cells creates a reverse electrical bias over the limiting sub-cell. In this particular tandem the PCDTBT:[70]PCBM cell is current limiting, but it displays a significant field-dependent current, and consequently the current density at reverse bias is higher than that under short-circuit conditions. Confirmation for this analysis comes from mathematically constructing the $J-V$ curve of the tandem from the $J-V$ curves of two single-junction cells that are identical to the tandem sub-cells, using Kirchhoff's law. The single-junction cells were measured under reduced light intensities that mimic the illumination densities of the sub-cell inside the tandem. This $J-V$ reconstruction yields exactly the same short-circuit current density (J_{sc} = 9.6 mA cm^{-2}, Figure 3b, dashed line).

To further improve the efficiency of organic solar cells, it is possible to add an additional photoactive layer of the same small band gap material, creating a triple-junction cell with a 1+2 configuration (Figure 3d). The motivation to add an additional junction is that in the tandem cell the J_{sc} is limited by the wide band gap front cell. Hence the small band gap back cell has the possibility of providing a surplus of photocurrent, but this is not used in the tandem. This limitation can be circumvented by splitting the small band gap sub-cell into two separate cells, a middle and back cell, as shown in Figure 3d. The middle and back sub-cells consist of the same photoactive layer and differ only in layer thickness to ensure that they both absorb an equal number of photons. By performing electrical–optical simulations on various triple configurations, using the characteristics of the individual photoactive layers, we established that such 1+2 triple-junction cells can provide increased efficiency compared to the tandem cells (Figure 3e and Table 2, predicted values). The increased V_{oc} of the triple junction outweighs the loss in J_{sc}. The optimal thicknesses for each of the three photoactive layers in the triple cell determined from the simulations were 125, 95, and 215 nm for the front, middle, and back cell respectively (Figure S12).

To test these predictions we fabricated triple-junction solar cells. Their average PCE among five nominally identical cells was 9.3%, and the best device gave PCE = 9.6%. The resulting $J-V$ characteristics and EQE measurements are shown in Figure 3e,f, and the data are collected in Table 2. The 1+2 triple-junction architecture represents a useful method to enhance the efficiency of tandem polymer solar cells with unbalanced sub-cells. As expected, the EQE in the triple-junction cell is reduced compared to that in the tandem cell because photons are absorbed in three instead of two layers, but the lower current is compensated by higher V_{oc} = 2.09 vs 1.48 V.

In summary, we demonstrate tandem and triple-junction polymer–fullerene solar cells with PCEs of 8.9% and 9.6%, respectively. The multi-junction cells use a new small band gap semiconducting polymer, PMDPP3T, with absorption in the near-infrared region up to 960 nm. Compared to the single-junction cells with the same layer thickness, the efficiency of the

dx.doi.org/10.1021/ja401434x | J. Am. Chem. Soc. 2013, 135, 5529–5532

optimized tandem and triple junctions is increased by as much as 50−60% by using highly complementary absorber layers. The 1+2 triple-junction architecture further enhances the performance of the tandem by exploiting the excess current generation of the nonlimiting sub-cell. The 1+2 configuration seems a valuable strategy to enhance the efficiency of tandem polymer solar cells with unbalanced sub-cells.

■ ASSOCIATED CONTENT

Supporting Information

Experimental details and characterization data. This material is available free of charge via the Internet at http://pubs.acs.org.

■ AUTHOR INFORMATION

Corresponding Author

r.a.j.janssen@tue.nl

Notes

The authors declare no competing financial interest.

■ ACKNOWLEDGMENTS

We thank S. Esiner and W. C. S. Roelofs for assistance and Konarka Technologies and Agfa for providing PCDTBT and Orgacon PEDOT:PSS. This work was performed in the framework of the Largecells and X10D projects that received funding from the European Commission's Seventh Framework Programme (Grant Agreement Nos. 261936 and 287818). The work was supported by the "Europees Fonds voor Regionale Ontwikkeling" in the Interreg IV-A project "Organext". The research forms part of the Solliance OPV programme.

■ REFERENCES

(1) He, Z. C.; Zhong, C. M.; Su, S. J.; Xu, M.; Wu, H. B.; Cao, Y. *Nat. Photon.* **2012**, *6*, 591−595.
(2) Zhang, F. L.; Bijleveld, J.; Perzon, E.; Tvingstedt, K.; Barrau, S.; Inganäs, O.; Andersson, M. R. *J. Mater. Chem.* **2008**, *18*, 5468−5474.
(3) Zhou, E. J.; Wei, Q. S.; Yamakawa, S.; Zhang, Y.; Tajima, K.; Yang, C. H.; Hashimoto, K. *Macromolecules* **2010**, *43*, 821−826.
(4) Perzon, E.; Zhang, F.; Andersson, M.; Mammo, W.; Inganäs, O.; Andersson, M. R. *Adv. Mater.* **2007**, *19*, 3308−3311.
(5) Xia, Y. J.; Wang, L.; Deng, X. Y.; Li, D. Y.; Zhu, X. H.; Cao, Y. *Appl. Phys. Lett.* **2006**, *89*, 081106.
(6) Zoombelt, A. P.; Fonrodona, M.; Wienk, M. M.; Sieval, A. B.; Hummelen, J. C.; Janssen, R. A. J. *Org. Lett.* **2009**, *11*, 903−906.
(7) Kim, J. Y.; Lee, K.; Coates, N. E.; Moses, D.; Nguyen, T. Q.; Dante, M.; Heeger, A. J. *Science* **2007**, *317*, 222−225.
(8) Gilot, J.; Wienk, M. M.; Janssen, R. A. J. *Adv. Mater.* **2010**, *22*, E67−E71.
(9) Dou, L. T.; You, J. B.; Yang, J.; Chen, C. C.; He, Y. J.; Murase, S.; Moriarty, T.; Emery, K.; Li, G.; Yang, Y. *Nat. Photon.* **2012**, *6*, 180−185.
(10) Dou, L. T.; Gao, J.; Richard, E.; You, J. B.; Chen, C. C.; Cha, K. C.; He, Y. J.; Li, G.; Yang, Y. *J. Am. Chem. Soc.* **2012**, *134*, 10071−10079.
(11) You, J.; Dou, L.; Yoshimura, K.; Kato, T.; Ohya, K.; Moriaty, T.; Emery, K.; Chen, C.-C; Li, G.; Yang, Y. *Nat. Commun.* **2013**, *4*, 1446.
(12) Blouin, N.; Michaud, A.; Leclerc, M. *Adv. Mater.* **2007**, *19*, 2295−2300.
(13) Sun, Y. M.; Takacs, C. J.; Cowan, S. R.; Seo, J. H.; Gong, X.; Roy, A.; Heeger, A. J. *Adv. Mater.* **2011**, *23*, 2226−2230.
(14) Wienk, M. M.; Turbiez, M.; Gilot, J.; Janssen, R. A. J. *Adv. Mater.* **2008**, *20*, 2556−2560.
(15) Yiu, A. T.; Beaujuge, P. M.; Lee, O. P.; Woo, C. H.; Toney, M. F.; Fréchet, J. M. J. *J. Am. Chem. Soc.* **2012**, *134*, 2180−2185.
(16) Bronstein, H.; Chen, Z. Y.; Ashraf, R. S.; Zhang, W. M.; Du, J. P.; Durrant, J. R.; Tuladhar, P. S.; Song, K.; Watkins, S. E.; Geerts, Y.; Wienk, M. M.; Janssen, R. A. J.; Anthopoulos, T.; Sirringhaus, H.; Heeney, M.; McCulloch, I. *J. Am. Chem. Soc.* **2011**, *133*, 3272−3275.
(17) Li, W. W.; Roelofs, W. S. C.; Wienk, M. A.; Janssen, R. A. J. *J. Am. Chem. Soc.* **2012**, *134*, 13787−13795.
(18) Bijleveld, J. C.; Zoombelt, A. P.; Mathijssen, S. G. J.; Wienk, M. M.; Turbiez, M.; de Leeuw, D. M.; Janssen, R. A. J. *J. Am. Chem. Soc.* **2009**, *131*, 16616−16617.
(19) Ye, L.; Zhang, S.; Ma, W.; Fan, B.; Guo, X.; Huang, Y.; Ade, H.; Hou, J. *Adv. Mater.* **2012**, *24*, 6335−6341.
(20) Fitzner, R.; Mena-Osteritz, E.; Mishra, A.; Schulz, G.; Reinold, E.; Weil, M.; Korner, C.; Ziehlke, H.; Elschner, C.; Leo, K.; Riede, M.; Pfeiffer, M.; Uhrich, C.; Bäuerle, P. *J. Am. Chem. Soc.* **2012**, *134*, 11064−11067.
(21) Chen, Y. H.; Lin, L. Y.; Lu, C. W.; Lin, F.; Huang, Z. Y.; Lin, H. W.; Wang, P. H.; Liu, Y. H.; Wong, K. T.; Wen, J. G.; Miller, D. J.; Darling, S. B. *J. Am. Chem. Soc.* **2012**, *134*, 13616−13623.
(22) Huang, F.; Wu, H. B.; Wang, D.; Yang, W.; Cao, Y. *Chem. Mater.* **2004**, *16*, 708−716.
(23) He, Z. C.; Zhang, C.; Xu, X. F.; Zhang, L. J.; Huang, L.; Chen, J. W.; Wu, H. B.; Cao, Y. *Adv. Mater.* **2011**, *23*, 3086−3089.
(24) He, Z.; Zhong, C.; Huang, X.; Wong, W.-Y.; Wu, H.; Chen, L.; Su, S.; Cao, Y. *Adv. Mater.* **2011**, *23*, 4636−4643.
(25) Gevaerts, V. S.; Furlan, A.; Wienk, M. M.; Turbiez, M.; Janssen, R. A. J. *Adv. Mater.* **2012**, *24*, 2130−2134.
(26) Beek, W. J. E.; Wienk, M. M.; Kemerink, M.; Yang, X. N.; Janssen, R. A. J. *J. Phys. Chem. B* **2005**, *109*, 9505−9516.
(27) Gilot, J.; Wienk, M. M.; Janssen, R. A. J. *Adv. Funct. Mater.* **2010**, *20*, 3904−3911.